# Seismic evidence of continental margin influence on the NinetyEast Ridge in the Bay of Bengal

Raphaele E. Moeremans, Satish C. Singh

AGU PUBLICATIONS

Geophysical Research Letters

RESEARCH LETTER
10.1002/2014GL061598

**Key Points:**
- Thick sediments are imaged on the eastern flank of the NER
- The northern segment of the NER was emplaced close to a continental margin
- Results are important for geodynamics, oil and gas generation, and subduction

**Supporting Information:**
- Readme
- Figure S1
- Figure S2
- Figure S3

**Correspondence to:**
R. E. Moeremans,
moeremans@ipgp.fr

**Citation:**
Moeremans, R. E., and S. C. Singh (2014), Seismic evidence of continental margin influence on the NinetyEast Ridge in the Bay of Bengal, *Geophys. Res. Lett.*, *41*, 7143–7150, doi:10.1002/2014GL061598.

Received 27 AUG 2014
Accepted 9 OCT 2014
Accepted article online 12 OCT 2014
Published online 31 OCT 2014

# Seismic evidence of continental margin influence on the NinetyEast Ridge in the Bay of Bengal

**Raphaele E. Moeremans[1] and Satish C. Singh[1]**

[1]Équipe de Géosciences Marines, Institut de Physique du Globe de Paris (CNRS, Paris Diderot, Sorbonne Paris Cité), Paris, France

**Abstract** The NinetyEast Ridge (NER), one of the most enigmatic features in the Indian Ocean, is covered by thick Bengal Fan sediment north of 9°N. We present seismic reflection data on the eastern flank of the NER, at 10°N, that show the presence of 4–5 km thick sediments beneath the Bengal Fan sediments. These sediments can be imaged up to 60 km beneath the Andaman fore-arc accretionary wedge, suggesting that the décollement lies above these sediments. The presence of thick sediments above the northernmost segment of the NER suggests that this segment was close to a continental margin during its emplacement. We propose that these sediments were deposited soon after the breakup of India and Antarctica, between 130 and 100 Ma, and might act as source rocks for oil and gas generation beneath recent Bengal Fan sediments. Furthermore, subducting thick sediments can significantly change the seismogenic behavior of the Andaman subduction zone.

## 1. Introduction

Extending for ~6000 km, the NinetyEast Ridge (NER) is the longest linear bathymetric feature in the Indian Ocean (Figure 1a). The NER intersects with the Broken Ridge in the south at 30°S. It is oriented NNE-SSW, roughly following the 90°E meridian, between 34°S and 18°N [*Krishna et al.*, 1999]. Its presence is further revealed by seismic reflection and gravity data up to 20°N [*Maurin and Rangin*, 2009]. Because the NER is buried under thick Bengal Fan sediments in the north, little is known about its emplacement history and nature north of 5°N.

The NER seems to have formed from hot spot volcanism at the Kerguelen hot spot, now located beneath the Kerguelen Plateau, and its interaction with the Wharton spreading center (WSC) near which the hot spot was often located [*Sager et al.*, 2010]. Initial activity at the Kerguelen hot spot (118–119 Ma [*Frey et al.*, 2003]) coincides with the breakup of eastern Gondwanaland into Australia-Antarctica and Greater India in the Early Cretaceous [*Curray et al.*, 1982; *Gopala Rao et al.*, 1997]. The NER followed the northward motion of the Indian Plate over the Kerguelen hot spot from the Late Cretaceous to the early Oligocene and ages northward [*Coffin et al.*, 2000; *Krishna et al.*, 1999]. Based on paleomagnetic data [*Pierce*, 1978; *Krishna et al.*, 2012], it was suggested that the NER was attached to the Indian Plate and both drifted rapidly northward, reaching a velocity of up to 20 cm/yr [*Jurdy and Gordon*, 1984; *Cande and Stegman*, 2011]. The formation of the NER ceased around ~42 Ma, when the large-scale reorganization of spreading centers moved the Kerguelen hot spot permanently beneath the Antarctica Plate.

The exposed portion of the NER between 30°S and 9°N has been divided into three morphologically distinct segments [e.g., *Royer et al.*, 1991; *Tiwari et al.*, 2003], mostly visible in gravity anomalies (Figure 1b). These different morphological expressions seem to be related to different geological settings during emplacement, more specifically to variations in the distance between the hot spot and the WSC, with the northern part having formed off ridge and the southern part near ridge [*Sager et al.*, 2010; *Royer et al.*, 1991]. Free-air gravity maps (Figure 1b) show a positive free-air gravity anomaly oriented N10E over the entire ridge until ~9°N, after which the anomaly shows a different character and is oriented slightly more to the east (N20E) up to ~18°N. The NER is suggested to be at an early stage of collision with the Andaman–Nicobar subduction system but may not have gone down beneath the fore arc yet [*Subrahmanyam et al.*, 2008].

The northernmost segment of the NER indents the Andaman–Nicobar segment of the Sumatra subduction zone around 8°N. The Andaman–Nicobar segment is an area of high seismic risk, as its entirety ruptured during the 26 December 2004 event ($M_w$ ~9.3). Subducting bathymetric highs, such as the NER, can significantly modify seismogenic behavior [e.g., *Cloos*, 1993; *Singh et al.*, 2011], as well as affect spreading processes in the back-arc basin. We use seismic reflection data from the northeastern flank of the NER, which is least studied, and beneath the Andaman fore-arc region, which we analyze to shed light upon the possible origin of the NER

  

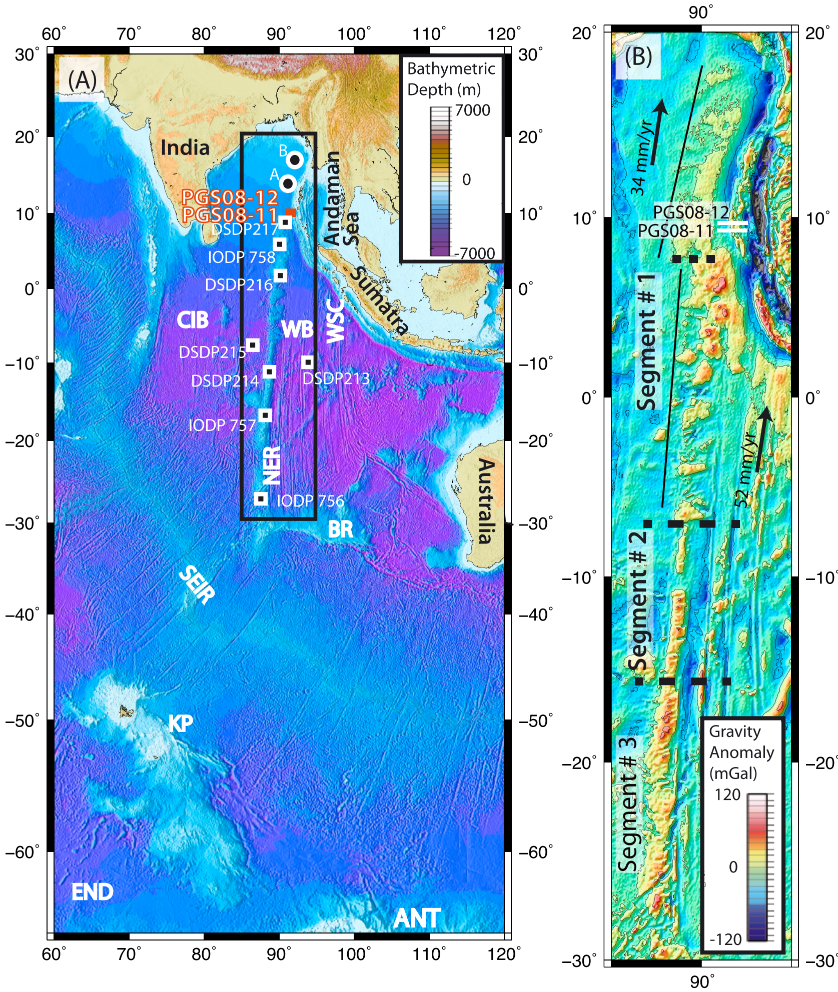


**Figure 1.** (a) High-resolution General Bathymetric Chart of the Oceans bathymetric map showing the NinetyEast Ridge (NER), the Andaman–Sumatra subduction zone, the Wharton Basin (WB), and the major features in the Central Indian Basin (CIB). IODP and DSDP drilling sites are shown by black and white squares. Five DSDP sites were drilled along the ridge (sites DSDP 213–DSDP 217). Three IODP sites also sample the crest of the ridge (IODP 756–758). Our two seismic reflection profiles are indicated by thick red lines. The locations of (A) *Samajdar et al.* [2013] and (B) *Maurin and Rangin* [2009] are marked by black and white circles. ANT = Antarctica, BR = Broken Ridge, EB = Elan Bank, END = Enderby Basin, KP = Kerguelen Plateau, SEIR = Southeast Indian Ridge, WB = Wharton Basin, and WSC = Wharton spreading center. (b) Gravity anomaly of the NER from *Sandwell et al.* [2013]. The three major morphological segments (1–3) are marked. The location of our seismic reflection profiles is marked by white lines. The plate motion vectors are shown by black arrows [*Prawirodirdjo and Bock*, 2004; *Gahalaut et al.*, 2006]. The black box in Figure 1a is the area shown in Figure 1b.

and its role in the subduction process. We provide a new interpretation for the origin of this segment of the NER, which has significant implications for the subduction processes in the area. The focus of this paper is on (1) identifying the nature of the layering observed on the subducting plate on the eastern flank of the NER and (2) proposing a process of emplacement by integrating the results of our interpretation with models for the evolution of the Indian Ocean Basin.

## 2. Seismic Data and Results

We present images from two seismic reflection profiles (Figures 2 and 3 and Figures S1 and S2 in the supporting information) across the deformation front of the Andaman–Sumatra subduction zone, from the subducting oceanic plate to the fore-arc high, around 10°N (Figure 1a). The data were acquired by Petroleum Geo-Services (PGS) in 2008, using an 8 km long streamer towed at 7.5 m water depth. The shot interval was 25 m, and the recording length was 9 s. The data were processed up to pre-stack-time migration,

  

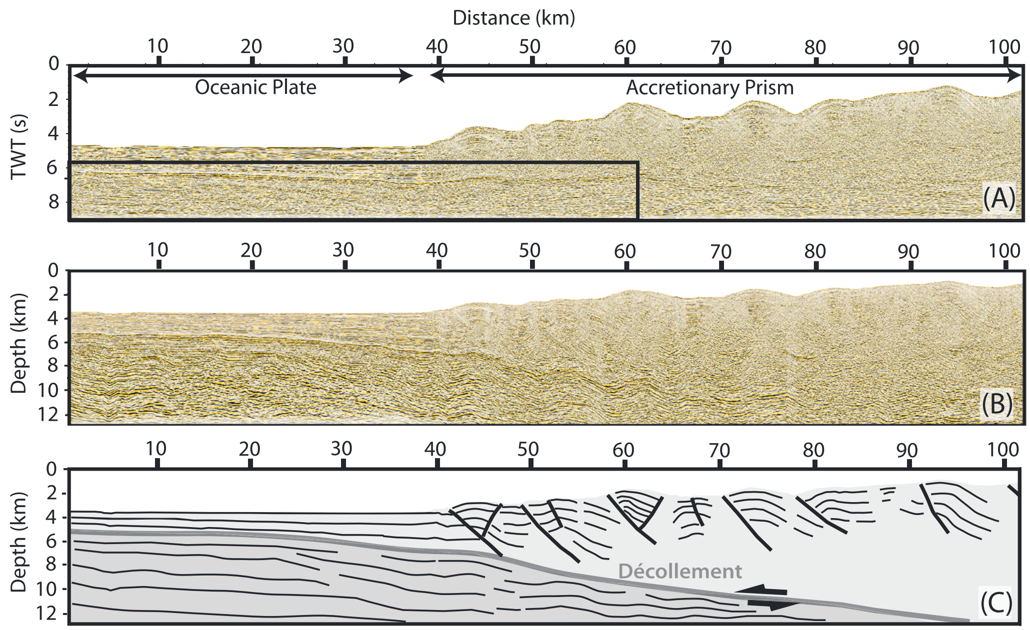


**Figure 2.** Seismic reflection profile PGS08-11 (a) in the time domain, (b) in depth domain, and (c) interpreted depth domain. The black box encloses the area shown in Figure 3b.

using conventional processing techniques [*Singh et al.*, 2013; *Moeremans et al.*, 2014]. Both profiles PGS08-11 (Figure 2 and Figure S1 in the supporting information) and PGS08-12 (Figure S2 in the supporting information) were shot orthogonally to the trench near 10°N and are 28 km apart. We also show a line drawing of a seismic profile shot over the NER at 13°N [*Samajdar et al.*, 2013] (Figure 3c).

Figure 2 shows the seismic images in both time and depth domains. The depth image was obtained by using a smoothed version of the interval velocity (Figure 4) estimated from the root-mean-square (RMS) stacking velocities provided by PGS, as well as the time images. Most of the images are therefore shown in the time domain, as one has to be cautious when interpreting the depth images alone, since the purpose of the velocities used was to produce the stacked time section. The seafloor of the oceanic plate on profile PGS08-11 is flat, at ~3.3 km (Figure 2b). A high-amplitude reflection at ~6 s separates the more recent Bengal Fan sediments above from the ~3 s thick subhorizontal reflections beneath. This high-amplitude reflection can be imaged for ~60 km beneath the accretionary prism and lies at the base of deformed accretionary sediments. A similar reflector is imaged on profile PGS08-12 (Figure 3a and Figure S2 in the supporting information), suggesting that these reflectors are at the top of the subducting plate, similarly to other areas of the Andaman–Sumatra subduction zone [*Moeremans et al.*, 2014]. These high-amplitude reflectors, visible seaward of the trench and up to 60 km beneath the accretionary wedge, mark an unconformity that seems to control the location of the subduction décollement.

These reflections are not multiples, as the multiple would arrive at ~9 s two-way time (TWT), and they do not mimic the seafloor, particularly beneath the frontal thrust. On profile PGS08-12 (Figure 3a), these reflectors onlap onto a convex crustal structure, visible right below the top of the subducting plate at 15 km from the start of the profile. On profile PGS08-11 (Figure 2 and Figure 3b and Figure S1 in the supporting information), this sequence of subhorizontal reflectors could be up to 5 km thick. Their character is very similar to the Bengal Fan sediments above but with higher amplitudes.

Figure 3c shows a line drawing of a seismic image over the NER at ~13°N. Similarly to the PGS profiles, we observe a strong reflector, similar in character to the top of the oceanic plate on the PGS profiles. Beneath this strong reflector is a thick (>2 s) sequence of reflections, which may correspond to the reflections observed along profile PGS08-11.

## 3. Discussion

The sequences of continuous linear reflections, observed below the high-amplitude reflectors on profiles PGS08-11 and PGS08-12, could either result from basaltic lava flows/sills associated with the NER or could be

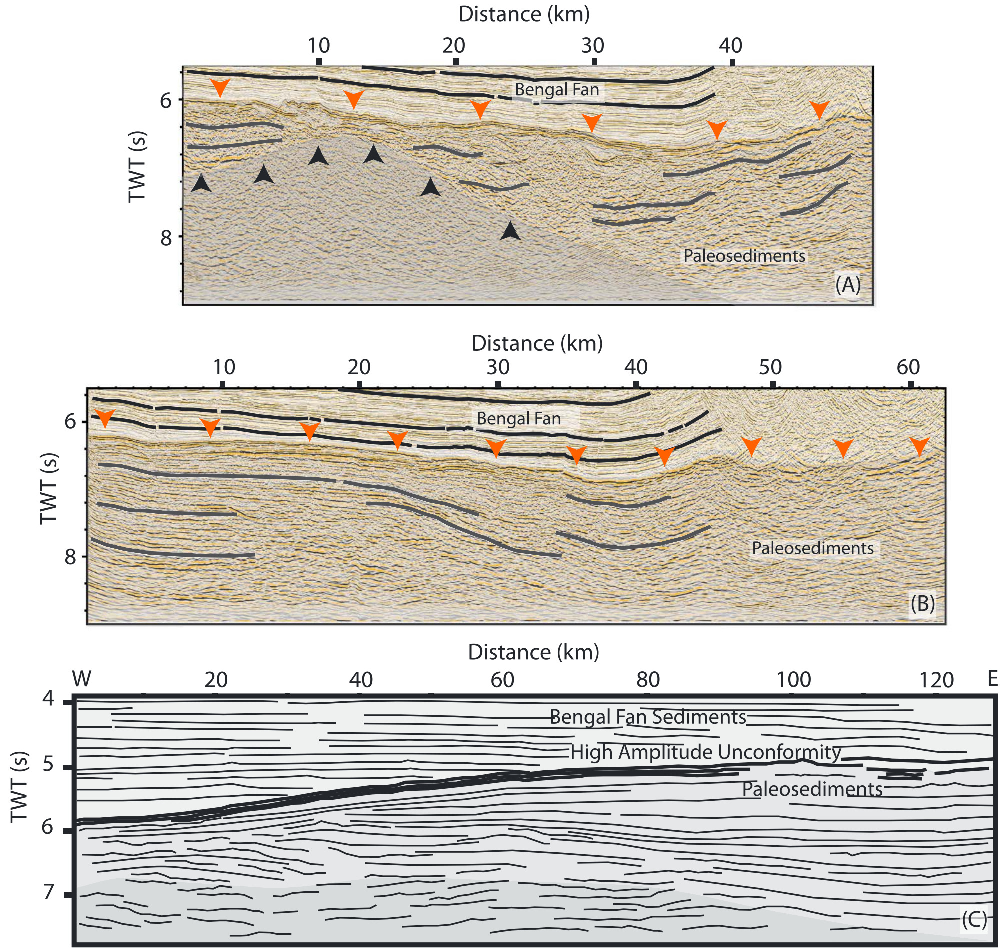


**Figure 3.** Blowups of the oceanic part of (a) PGS08-12 and (b) PGS08-11. The orange arrows indicate the high-amplitude unconformity, which controls the position of the subduction décollement. The black arrows in Figure 3a show the igneous body on which the reflectors onlap. (c) Line drawing of an E-W seismic reflection profile around 13°N modified from *Samajdar et al.* [2013].

old compacted sediments. Extensive basaltic lava flows are often produced during continental breakup. Basalt flows are, however, difficult to image using seismic methods [e.g., *Fliedner and White*, 2001] because (1) the highly reflective top of the basalt scatters a significant part of the incident seismic energy and (2) basalt layers preferentially absorb higher frequencies in the incident wave and degrade the image at depth. Additionally, large-volume extrusive basaltic formations can have different morphologies and seismic properties depending on the eruption type and emplacement environment. Our observations from profiles PGS08-11 and PGS08-12 could be landward flows [*Planke et al.*, 2000], which are characterized by a strong, fairly smooth top reflection and internal and disrupted subparallel internal reflections. The basal boundary may be identified as a negative-polarity reflection on high-resolution data, but frequently, no reflectors are identified below.

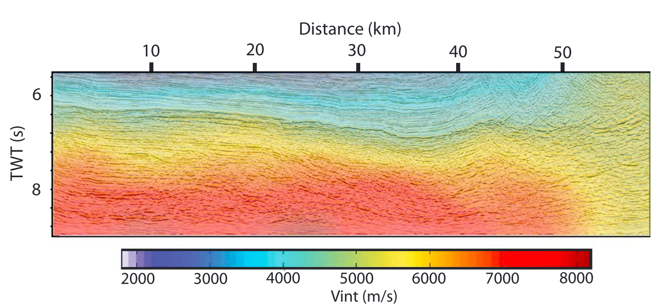


**Figure 4.** Interval velocities for the oceanic part of PGS08-11 used to produce the depth-converted image shown in Figure 2b.

Drilling of the landward flows off Western Australia, and in the north Atlantic, recovered subaerially emplaced flood basalts, with no or thin interbedded sediment layers [*Planke et al.*, 2000]. Similarly, offshore the Osa Peninsula, observed upper crustal layering of the Cocos Ridge flank has been interpreted to consists of 2 km thick basaltic flows [*von Huene et al.*, 2000]. An average velocity of 4.4 km/s, correlating with seismic reflection data, indicates flow basalts with interbedded sediments [*Walther*, 2003].

Therefore, although basement layering and some seaward dipping reflections associated with basaltic lava intrusions have been imaged [*Joppen and White*, 1990; *Planke et al.*, 2000; *von Huene et al.*, 2000], it would be difficult to image a 5 km thick lava flow sequence over a distance of 100 km using seismic methods [*Masoomzadeh et al.*, 2010], specifically beneath 10–15 km thick accretionary wedge sediments (Figure 2a).

From the interval velocities, which we computed from the RMS stacking velocities (Figure 4), it is difficult to discriminate between these two possible interpretations, as the velocities (5–7 km/s) are consistent with both igneous rocks and highly compacted sediments. These velocities are, however, poorly constrained and may contain a large component of error particularly at depth, as their purpose was to produce the stacked time section. Typical velocities for igneous crust are ~5–8 km/s [e.g., *Spudich and Orcutt*, 1980], but *Minshull and White* [1989] find velocities of up to 5 km/s in compacted sediments at depths within the sediments of 4–5 km. Velocities at greater depths could thus be higher, as observed in our profiles at 6–8 km depth.

We thus interpret these reflections as a thick section of old compacted sediments, and the high-amplitude reflector that represents the top of the subducting oceanic plate at ~6 s TWT as an unconformity between the Bengal Fan sediments above and thick paleosediments below. Such unconformities have been observed elsewhere in the Indian Ocean Basin [*Gopala Rao et al.*, 1994] and could correspond to the deposition of pelagic sediments between the older sediments (100 Ma) and the Bengal Fan (~42 Ma). Alternatively, this sequence of reflection may represent a thick early breakup basaltic flow [*Planke et al.*, 2000]. In both cases, the paleosediments or early breakup lava flows could be lie above either thinned continental crust or oceanic crust, which has strong implications for subduction processes and back-arc volcanism.

Other seismic studies further north along the NER near 16°N [*Maurin and Rangin*, 2009] and 13°N [*Samajdar et al.*, 2013] (Figure 3c) have noted the presence of thick paleosediments on the top and on the flanks of the northern segment of the NER. *Samajdar et al.* [2013] identified a major unconformity between the Bengal Fan sediments and the underlying paleosediments in E-W seismic reflection profiles acquired between 13°N and 15°N and 90 and 92°E (Figure 3c), which they interpret as the Cretaceous/Tertiary boundary. The combination of these observations suggests that a large portion of the northern segment of the NER is covered and flanked by thick paleosediments, over hundreds of kilometers, along the ridge in the N-S direction. In order to have 5 to 6 km (Figure 2c; obtained from 3 s TWT (Figure 2a) and the velocities shown in Figure 4) of deposited sediment, this segment of the ridge must have been emplaced close to a continent rather than in the deep ocean. The sediments we image at 10°N, and the ones visible in other studies up to 16°N, are expected to be older than the Late Cretaceous ones found in Deep Sea Drilling Project (DSDP) and International Ocean Discovery Program (IODP) sites further to the south (Figure 1a).

Plate reconstruction models can help better constrain the location and timing of deposition for these paleosediments. The northern segment of the NER must have been emplaced during the rifting and northward drifting of India before ~84 Ma, because magnetic anomaly 34 has been observed in both the Central Indian Basin (CIB) and the Wharton Basin (WB), but so far, no consensus has been reached regarding the breakup of India and Antarctica due to the absence of clear and continuous magnetic anomalies off eastern India. Indeed, the subduction of the Neothethyan and Proto-Indian Ocean lithosphere destroyed information about the drift path of the Indian continental block before chron C34 (~83.5 Ma) [e.g., *Seton et al.*, 2012]. Some models associate the breakup with the first occurrence of the Kerguelen Plateau at 118–119 Ma (Figure S3b in the supporting information) [*Royer and Coffin*, 1992; *Banerjee et al.*, 1995; *Jokat et al.*, 2010], while others associate it with older identified magnetic anomalies off of Antarctica, M0–M4, and up to M10 at ~133 Ma (Figure S3b in the supporting information) [*Ramana et al.*, 2001; *Desa et al.*, 2006; *Gaina et al.*, 2007; *Gibbons et al.*, 2013]. Seafloor spreading anomalies from M9 to M0 (130 Ma to 120.4 Ma) were identified in the eastern Enderby Basin, which is the conjugate margin of the Bay of Bengal basin [*Gaina et al.*, 2007]. An alternative interpretation establishes seafloor spreading at ~127 Ma, after identifying magnetic anomalies M4 to M0 (~126.7–120.4 Ma) [*Gibbons et al.*, 2013]. In both cases, opening between India and Antarctica occurred around 130 Ma. Because of this, we suggest ~130 Ma as the upper limit of crustal age in the northern segment of the NER. Magnetic anomalies document a major change in direction of spreading along western Australian margin at 100 Ma, leading to a change in

  

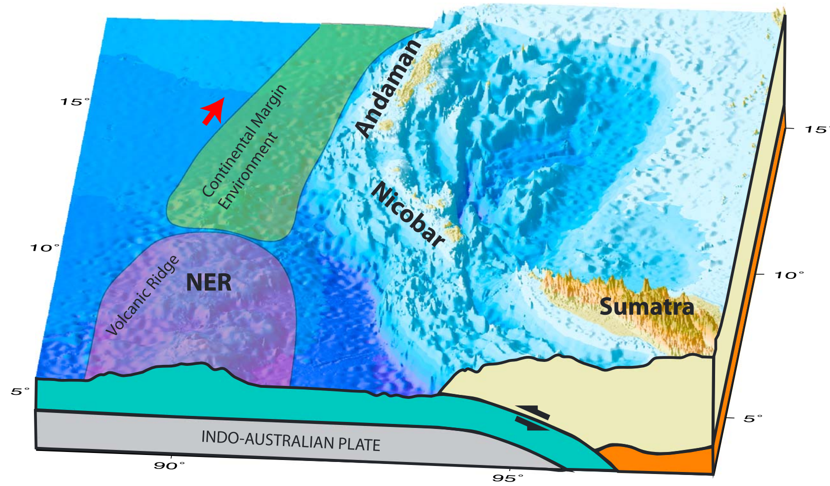


**Figure 5.** Block diagram summarizing the emplacement setting of the northernmost segment of the NER.

motion of the Indian Plate, and establishing spreading in the WB, and suggest that from this time onward, India started to move rapidly northward [*Müller et al.*, 1997; *Heine et al.*, 2004]. At this point, India would have been too far from a continental margin, and we thus take 100 Ma to correspond to the lower limit of crustal age. We therefore propose that the northern segment of the NER was emplaced between ~130 and 100 Ma.

Figure S3 in the supporting information summarizes the evolution of the NER and rifting of India. Seafloor spreading separating Greater India from Australia-Antarctica started at ~136 Ma northwest of Australia, reaching southern India at ~127 Ma [*Gibbons et al.*, 2013]. The hot spot formed a large portion of the Kerguelen Plateau during the mid-Cretaceous near the intersection of the Indian, Antarctica, and Australian continental blocks, when they were still close to their Gondwanaland positions. The northern segment of the NER started to form over the hot spot during the initiation of rifting. The hot spot emplaced basalts forming the NER on the northward migrating Indian Plate and the Kerguelen Plateau on the Antarctic Plate. Some Cretaceous basalts of the Kerguelen Plateau have a continental signature [*Frey et al.*, 2002], which is not observed on basalts collected on the NER [*Frey and Weis*, 1995]. However, no basalts have been collected on the NER north of 9°N, and the basalts in its northern segment could have a similar continental influence. Furthermore, Ocean Drilling Program Leg 183 drilled the Elan Bank, on the western side of the south Kerguelen Plateau (Figure 1), proving it to be continental with a minimum age of 108 Ma [*Frey et al.*, 2003]. *Gaina et al.* [2007] showed that this microcontinent was detached from India and transferred to the Antarctic crust ~120 Ma. Such an emplacement setting has implications for oil and gas production, as oceanic anaerobic events have been reported globally during the Cretaceous period. In addition, the concentrations of high terrigenous organic carbon black beds have been reported in the Cretaceous sections of ocean basins, including the Indian Ocean [*Samajdar et al.*, 2013].

The presence of thick sediments over rough NER basement topography would have a significant effect on the friction coefficient at the plate interface and hence the coupling. The sediment-sediment plate interface would increase the area of the stable part of the wedge. The rupture areas of large events, such as the 2010 $M_w$ 8.8 Maule earthquake, generally coincide with the stable areas of the fore arc. The presence of low effective friction material due to the sediment-sediment megathrust interface that extends up to 60 km beneath the fore arc (Figure 2b) could explain the updip extension and large northward propagation of the coseismic rupture of the 2004 Sumatra–Andaman event.

Based on a seismic reflection and refraction study, *Rangin et al.* [2013] suggested the presence of thick oceanic crust or thinned continental crust beneath the Bay of Bengal. Surface wave studies also indicated the possible presence of thinned Indian continental crust in the northern part of the Bengal Basin [*Brune and Singh*, 1986; *Mitra et al.*, 2005]. It is therefore possible that the northern segment of the NER was emplaced on the Indian continental crust, similarly to other continental fragments that were later transferred to the Antarctic Plate, and the thick Createaceous sediments on the flank and above the NER were deposited over this thinned continental crust during the early breakup of India and Antarctica. Buoyant thinned continental crust would result in a shallower dip of the first segment of the slab and inhibit the subduction process. The steep dip of the subducting slab [*Shapiro et al.*, 2008] beneath the Andaman Sea might be due to a tear in the subducted oceanic lithosphere at depth due to buoyant shallow-dipping sedimented crust beneath the fore arc.

## 4. Conclusions

We have imaged a thick layered sequence below the Bengal Fan sediments on the eastern flank of the NER that we interpret as Early Cretaceous paleosediments. The thickness of these paleosediments suggests that the northern segment of the NER was emplaced close to a continental margin setting (Figure 5) between 130 and 100 Ma. The thick Cretaceous sediments beneath the Bengal Fan sediments could act as source rocks for oil and gas generation. Additionally, these sediments over thinned continental crust could alter the frictional properties at the décollement and thus the coupling at the subduction interface. Sedimented, buoyant thinned continental crust would also inhibit the subduction.

**Acknowledgments**
We would like to thank Petroleum Geo-Services for providing the Andaman Sea data, as well as Jérôme Dyment and Jean Besse for the discussions on the geodynamics of the Indian Ocean. We would like to thank Kirk McIntosh and Carmen Gaina for their very thorough review of the paper. Seismic reflection data to support this article are from Petroleum Geo-Services and cannot be released. The full uninterpreted images of the profiles used in Figure 3 are, however, available in Figures S1 and S2 in the supporting information. This is an Institut de Physique du Globe de Paris contribution 3577.

The Editor thanks Kirk McIntosh, Carmen Gaina, and an anonymous reviewer for their assistance in evaluating this paper.

## References

Banerjee, B., J. Sengpta, and P. K. Banerjee (1995), Signals of Barremian (116 Ma) or younger oceanic crust beneath the Bay of Bengal along 14 N latitude between 81E and 93E, *Mar. Geol.*, *128*, 17–23.

Brune, J. N., and D. D. Singh (1986), Continent-like crustal thickness beneath the Bay of Bengal Sediments, *Bull. Seismol. Soc. Am.*, *76*, 191–203.

Cande, S. C., and D. R. Stegman (2011), Indian and African plate motions driven by the push force of the Réunion plume head, *Nature*, *475*, 47–52.

Cloos, M. (1993), Lithospheric buoyancy and collisional orogenesis: Subduction of oceanic plateaus, continental margins, island arcs, spreading ridges, and seamounts, *Geol. Soc. Am. Bull.*, *105*(6), 715–737.

Coffin, M. F., M. S. Pringle, R. A. Duncan, T. P. Gladczenko, M. Storey, R. D. Müller, and L. A. Gahagan (2000), Kerguelen hotspot magma output since 130Ma, *J. Petrol.*, *43*, 1121–1139.

Curray, J. R., F. J. Emmel, D. G. Moore, and R. W. Raitt (1982), Structure, tectonics, and geological history of the northeastern Indian Ocean, in *The Ocean Basins and Margins*, pp. 399–450, Springer, New York.

Desa, M., M. V. Ramana, and T. Ramprasad (2006), Seafloor spreading magnetic anomalies south of Sri Lanka, *Mar. Geol.*, *229*, 227–240.

Fliedner, M. M., and R. S. White (2001), Seismic structure of basalt flows from surface seismic data, borehole measurements, and synthetic seismogram modeling, *Geophysics*, *66*, 1925–1936.

Frey, F. A., and D. Weis (1995), Telporal evolution of the Kerguelen plume: Geochemical evidence from ~38 to 82 Ma lavas forming the Ninetyeast Ridge, *Contrib. Mineral Petrol.*, *121*, 12–28.

Frey, F. A., D. Weis, A. Y. Borisova, and G. Xu (2002), Involvement of continental crust in the formation of the Cretaceous Kerguelen Plateau: New perspectives from ODP Leg 120 Sites, *J. Petrol.*, *43*, 1207–1239.

Frey, F. A., M. F. Coffin, P. J. Wallace, and P. G. Quilty (Eds.) (2003), Proceedings of the Ocean Drilling Program, Sci. Results, vol. 183: College Station, Tex. (Ocean Drilling Program).

Gahalaut, V. K., B. Nagarajan, J. K. Catherine, and S. Kumar (2006), Constraints on 2004 Sumatra–Andaman earthquake rupture from GPS measurements in Andaman–Nicobar Islands, *Earth Planet. Sci. Lett.*, *242*(3), 365–374.

Gaina, C., R. D. Müller, B. Brown, and T. Ishihara (2007), Breakup and early seafloor spreading between India and Antarctica, *Geophys. J. Int.*, *170*, 151–169.

Gibbons, A. D., J. M. Whittaker, and R. D. Müller (2013), The breakup of East Gondwana: Assimilating constraints from Cretaceous ocean basins around India into a best-fit tectonic model, *J. Geophys. Res. Solid Earth*, *118*, 808–822, doi:10.1002/jgrb.50079.

Gopala Rao, D., et al. (1994), Analysis of multi-channel seismic reflection and magnetic data along 13°N latitude across the Bay of Bengal, *Mar. Geophys. Res.*, *16*, 225–236.

Gopala Rao, D., K. S. Krishna, and D. Sar (1997), Crustal evolution and sedimentation history of the Bay of Bengal since the Cretaceous, *J. Geophys. Res.*, *102*(B8), 17,747–17,768, doi:10.1029/96JB01339.

Heine, C., R. D. Müller, and C. Gaina (2004), Reconstructing the Lost Eastern Tethys Ocean Basin: Convergence history of the SE Asian Margin and marine gateways, in *Continent-Ocean Interactions in Southeast Asia*, *Geophys. Monogr. Ser.*, vol. 1149, edited by P. Clift et al., AGU, Washington, D. C.

Jokat, W., Y. Nogi, and V. Leinweber (2010), New aeromagnetic data from the western Enderby Basin and consequences for Antarctic-India break-up, *Geophys. Res. Lett.*, *37*, L21311, doi:10.1029/2010GL045117.

Joppen, M., and R. S. White (1990), The structure and subsidence of Rockall Trough from two ship seismic experiments, *J. Geophys. Res.*, *95*, 19,821–19,837, doi:10.1029/JB095iB12p19821.

Jurdy, D. M., and R. G. Gordon (1984), Global plate motions relative to the hotspots 64 to 56 Ma, *J. Geophys. Res.*, *89*, 9927–9936.

Krishna, K. S., D. Gopala Rao, L. V. Subba Raju, and A. K. Chaubey (1999), Paleocene on spreading-axis hotspot volcanism along the Ninetyeast Ridge: An interaction between the Kerguelen hotspot and the Wharton spreading center: Proceedings of the Indian Academy of Science, *Earth Planet. Sci.*, *108*, 255–267.

Krishna, K. S., H. Abraham, W. W. Sager, M. S. Pringle, F. Frey, D. Gopala Rao, and O. V. Levchenko (2012), Tectonics of the Ninetyeast Ridge derived from spreading records in adjacent oceanic basins and age constraints of the ridge, *J. Geophys. Res.*, *117*, B04101, doi:10.1029/2011JB008805.

Masoomzadeh, H., P. Barton, and S. C. Singh (2010), Nonstretch moveout correction of long offset multichannel seismic data for subbasalt imaging: Example from the North Atlantic, *Geophysics*, *75*, R83–R91.

Maurin, T., and C. Rangin (2009), Impact of the 90°E ridge at the Indo-Burmese subduction zone imaged from deep seismic reflection data, *Mar. Geol.*, *266*, 143–155.

Minshull, T., and R. White (1989), Sediment compaction and fluid migration in the Makran accretionary prism, *J. Geophys. Res.*, *94*(B6), 7387–7402, doi:10.1029/JB094iB06p07387.

Mitra, S., K. Priestley, A. K. Bhattacharyya, and V. K. Gaur (2005), Crustal structure and earthquake focal depths beneath northeastern India and southern Tibet, *Geophys. J. Int.*, *160*(1), 227–248.

Moeremans, R., S. C. Singh, M. Mukti, J. McArdle, and K. Johansen (2014), Seismic images of structural variations along the deformation front of the Andaman-Sumatra subduction zone: Implications for rupture propagation and tsunamigenesis, *Earth Planet. Sci. Lett.*, *386*, 75–85.

Müller, R. D., W. R. Roest, J. Y. Royer, L. M. Gahagan, and J. G. Sclater (1997), Digital isochrons of the world's ocean floor, *J. Geophys. Res.*, *102*, 3211–3214, doi:10.1029/96JB01781.

Pierce, J. W. (1978), The northward motion of India since the Late Cretaceous, *Geophys. J. R. Astron. Soc.*, *52*, 277–311.

Planke, S., P. A. Symonds, E. Alvestad, and J. Skogseid (2000), Seismic volcanostratigraphy of large-volume basaltic extrusive complexes on rifted margins, *J. Geophys. Res.*, *105*, 19,335–19,351, doi:10.1029/1999JB900005.

Prawirodirdjo, L., and Y. Bock (2004), Instantaneous global plate motion model from 12 years of continuous GPS observations, *J. Geophys. Res.*, *109*, B08405, doi:10.1029/2003JB002944.

Ramana, M. V., T. Ramprasad, and M. Desa (2001), Seafloor spreading magnetic anomalies in the Enderby Basin, East Antarctica, *Earth Planet. Sci. Lett.*, *191*, 241–255.

Rangin, C., T. Maurin, and F. Masson (2013), Combined effects of Eurasia/Sunda oblique convergence and East-Tibetan crustal flow on the active tectonics of Burma, *J. Asian Earth Sci.*, *76*, 185–194.

Royer, J. Y., and M. F. Coffin (1992), Jurassic to Eocene plate tectonic reconstructions in the Kerguelen Plateau region, *Proc. Ocean Drill. Program Part B Sci. Results.*, *120*, 917–928.

Royer, J.-Y., J. W. Peirce, and J. K. Weissel (1991), Tectonic constraints on the hotspot formation of Ninetyeast Ridge, *Proc. Ocean Drill. Program Part B Sci. Results.*, *121*, 763–775.

Sager, W. W., C. F. Paul, K. S. Krishna, M. Pringle, A. E. Eisin, F. A. Frey, D. Gopala Rao, and O. Levchenko (2010), Large fault fabric of the Ninetyeast Ridge implies near-spreading ridge formation, *Geophys. Res. Lett.*, *37*, L17304, doi:10.1029/2010GL044347.

Samajdar, C., A. Sengupta, and R. Kumar (2013), Ninety Degree East Ridge and hydrocarbon prospectivity of West Andaman area, paper presented at 10th Biennial International Conference and Exposition, Society of Petroleum Geophysicists, Kochi, India.

Sandwell, D. T., E. Garcia, K. Soofi, P. Wessel, and W. H. F. Smith (2013), Towards 1 mGal Global Marine Gravity from CryoSat-2, Envisat, and Jason-1, *The Leading Edge*, *32*, 892–899, doi:10.1190/tle32080892.1.

Seton, M., et al. (2012), Global Continental and ocean basin reconstructions since 200 Ma, *Earth Sci. Rev.*, *113*, 212–270.

Shapiro, N. M., M. H. Ritzwoller, and E. R. Engdahl (2008), Structural context of the great Sumatra-Andaman Islands earthquake, *Geophys. Res. Lett.*, *35*, L05301, doi:10.1029/2008GL033381.

Singh, S. C., et al. (2011), Aseismic zone and earthquake segmentation associated with a deep subducted seamount in Sumatra, *Nat. Geosci.*, *4*(5), 308–311.

Singh, S. C., R. Moeremans, J. McArdle, and K. Johansen (2013), Seismic images of the sliver strike-slip fault and back thrust in the Andaman-Nicobar region, *J. Geophys. Res. Solid Earth*, *118*, 5208–5224, doi:10.1002/jgrb.50378.

Spudich, P., and J. Orcutt (1980), A new look at the seismic velocity structure of oceanic crust, *Rev. Geophys. Space Phys.*, *18*(3), 627–645.

Subrahmanyam, C., R. Gireesh, S. Chand, K. A. Kamesh Raju, and D. Gopala Rao (2008), Geophysical characteristics of the Ninetyeast Ridge – Andaman Island Arc/Trench convergent zone, *Earth Planet. Sci. Lett.*, *266*, 29–45.

Tiwari, V. M., M. Diament, and S. C. Singh (2003), Analysis of satellite gravity and bathymetry data over Ninety-East Ridge: Variation in the compensation mechanism and implication for emplacement process, *J. Geophys. Res.*, *108*(B2), 2109, doi:10.1029/2000JB000047.

von Huene, R., C. R. Ranero, W. Weinrebe, and K. Honz (2000), Quaternary convergent margin tectonics of Costa Rica, segmentation of the Cocos Plate, and Central American volcanism, *Tectonics*, *19*, 314–334, doi:10.1029/1999TC001143.

Walther, C. H. E. (2003), The crustal structure of the Cocos ridge off Costa Rica, *J. Geophys. Res.*, *108*(B3), 2136, doi:10.1029/2001JB000888.

  